

# Non-Local Quantum Gates: a Cavity-Quantum-Electro-Dynamics implementation

M. Paternostro and M. S. Kim

*School of Mathematics and Physics, The Queen's University, Belfast BT7 1NN, United Kingdom*

G. M. Palma

*Dipartimento di Tecnologie dell'Informazione, Universita' di Milano, Via Bramante 65, 26013 Crema, Italy and  
NEST & INFN*

(Dated: October 30, 2018)

The problems related to the management of large quantum registers could be handled in the context of distributed quantum computation: unitary non-local transformations among spatially separated local processors are realized performing local unitary transformations and exchanging classical communication. In this paper, we propose a scheme for the implementation of universal non-local quantum gates such as a controlled-NOT (CNOT) and a controlled-quantum phase gate (CQPG). The system we have chosen for their physical implementation is a Cavity-Quantum-Electro-Dynamics (CQED) system formed by two spatially separated microwave cavities and two trapped Rydberg atoms. We describe the procedures to follow for the realization of each step necessary to perform a specific non-local operation.

PACS numbers: 03.67.Hk, 42.50.-p, 03.67.-a, 03.65.Bz

## I. INTRODUCTION

One of the major problems in the experimental implementation of large scale quantum computing devices is scalability, i.e. the physical control at microscopic level of a large number of quantum subsystems. In particular the destructive effects of decoherence grow with the size of the register [1]. Furthermore, undesired interactions among qubits of the same quantum register settle in an uncontrollable way [2, 3]. One possible solution to this problem could be distributed quantum computing. In this architecture a quantum computer is thought as a network of spatially separated devices, which we call *local processors*, each operating on a small number of qubits [4]. Such a design of a quantum computer has recently become particularly stimulating in view of the papers by Eisert *et al.* [5] and by Collins *et al.* [6]. In these works, the minimal amount of classical and quantum resources needed to realize a general non-local unitary transformation is investigated. In the case of two-qubits gates, two bits of classical communication and the maximally entangled state of a shared pair of qubit (*ebit*) are proved to be necessary and sufficient resources to implement a *controlled-U* gate [5]. In particular, in ref. [5], a theoretical protocol for the optimal implementation of a non-local controlled-NOT gate (CNOT) is described. This result is relevant since CNOT and single qubit operations constitute an adequate set for quantum computation [7, 8, 9, 10, 11]. We have summarized the protocol, using quantum circuit notation, in Fig. 1.

In this paper we propose an experimental scheme for the physical implementation of a non-local CNOT (according to the protocol proposed in ref. [5]) and of a non-local controlled-quantum phase gate (CQPG) in a Cavity-Quantum-Electro-Dynamics (CQED) set-up.

The paper is structured as follows: in section II we describe the protocol of ref. [5] for the local implementation

of a non-local CNOT and we show how to modify it to obtain a non-local control quantum phase gate. This latter is a relevant result as well, because the set of quantum gates that comprehends CQPG and single qubit rotations is universal for quantum computation [7, 8, 9]. Section III is devoted to a brief description of the experimental set-up we propose in order to implement these non-local gates. A short summary of the features of the interactions of a two level atom with a single mode of a cavity field is presented. We also describe an approach to the interaction of the atom with an external classical pulse. In sections IV and V we analyze in detail each step that compose the experimental scheme for the physical realization of the non-local CNOT and CQPG. We show how they are realizable in a CQED system including the description of a procedure for the preparation of the computational register and we comment on the way to obtain the required ebit. Every *local operation* is analyzed in full detail.

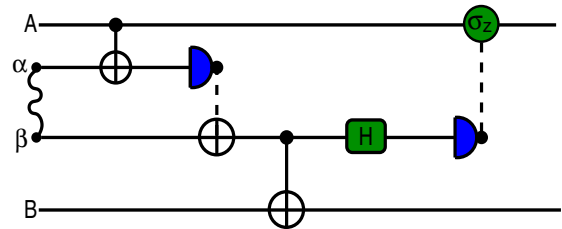


FIG. 1: Quantum circuit for a non-local CNOT gate realized using a shared ebit and two classical bits of communication. In this scheme,  $A$  is the control qubit and  $B$  is the target qubit. The joined state of qubits  $\alpha$  and  $\beta$  encodes the needed ebit (entanglement is represented by the wavy line). Classical communication is represented by dashed lines and symbols for CNOT operation, Hadamard transform and Pauli  $\sigma_z$  operator are shown. The measurements performed on the atomic qubit are schematically represented by detectors.

## II. THE THEORETICAL PROTOCOLS

In this section we briefly outline the protocol proposed by Eisert *et al.* [5]. We also show how the protocol can be modified to get a non-local CQPG.

Qubits  $A$  and  $B$  are, respectively, the control and the target of the non-local CNOT while  $\alpha$  and  $\beta$  are two auxiliary qubits encoding an ancillary ebit. Alice (Bob) has access only to qubits  $A$  and  $\alpha$  ( $B$  and  $\beta$ ). We assume that the initial state of qubits  $A$  and  $B$  is

$$|\varphi_{in}\rangle_A \otimes |\varphi_{in}\rangle_B = (a|1\rangle + b|0\rangle)_A \otimes (c|1\rangle + d|0\rangle)_B \quad (1)$$

while the ebit is set in the Bell state  $\frac{1}{\sqrt{2}}(|01\rangle + |10\rangle)_{\alpha\beta}$  (to optimize the fidelity of the non-local CNOT the joint state of  $\alpha$  and  $\beta$  must be a maximally entangled state [12]). The protocol can be read easily from Fig. 1. First of all Alice performs a local CNOT $_{A\alpha}$  where  $A$  is the control and  $\alpha$  is the target followed by an orthogonal measurement on  $\alpha$ . This transfers entanglement from qubits  $\alpha + \beta$  to qubits  $A + \beta$ . Bob then uses the classical information on the measurement result of qubit  $\alpha$  to act on qubit  $\beta$ : if the outcome of Alice's measurement is  $|1\rangle_\alpha$ , Bob applies a NOT on qubit  $\beta$  while he applies  $\mathbf{1}$  if Alice detects  $|0\rangle_\alpha$ . This gives the following state:

$$ac|111\rangle_{A\beta B} + ad|110\rangle_{A\beta B} + bc|001\rangle_{A\beta B} + bd|000\rangle_{A\beta B}. \quad (2)$$

Now, Bob first applies a CNOT $_{\beta B}$  followed by a Hadamard transform on qubit  $\beta$  and then detects its state. Depending on the measurement outcome, the state of  $A + B$  is projected onto two different states. If Bob detects  $|0\rangle_\beta$ , the state of system  $A + B$  is exactly what we expect from a CNOT $_{AB}$  applied on the initial state of the  $A + B$  system. If, on the other hand,  $|1\rangle_\beta$  is detected Alice applies the Pauli  $\sigma_z$  operator to qubit  $A$ , shifting the phase of  $|1\rangle_A$  by  $\pi$  and leaving  $|0\rangle_A$  unaltered. This gives the desired output state

$$ad|11\rangle_{AB} + ac|10\rangle_{AB} + bc|01\rangle_{AB} + bd|00\rangle_{AB}. \quad (3)$$

It is worth pointing out that the protocol works not only for the product input states of  $A + B$  considered here but also for entangled input ones.

With a minor change, the protocol can be modified to implement a non-local CQPG defined in the computational basis of qubits  $A, B$  as

$$\begin{aligned} |00\rangle &\rightarrow |00\rangle & |01\rangle &\rightarrow e^{i\phi} |01\rangle \\ |10\rangle &\rightarrow |10\rangle & |11\rangle &\rightarrow |11\rangle. \end{aligned} \quad (4)$$

Indeed it is enough to substitute the CNOT $_{\beta B}$  gate shown in Fig. 1 with a CQPG $_{\beta B}$ . A straightforward calculation shows that the overall effect of such modified circuit is the desired CQPG $_{AB}$ .

## III. THE PHYSICAL SYSTEM

The experimental set-up we propose in this paper is schematically shown in Fig. 2. Within each of two spatially separated high- $Q$  millimeter-wave cavities a single Rydberg atom is trapped. The angular frequency of each cavity mode is supposed to be nearly resonant with the transition frequency between two Rydberg levels of the respective atom so that the atoms can be modeled as two-level systems. Let us call  $|g\rangle, |e\rangle$  respectively the ground and the excited atomic state. Qubits  $A$  and  $B$  are encoded in the vacuum and one photon state  $\{|0\rangle, |1\rangle\}_A$  and  $\{|0\rangle, |1\rangle\}_B$  of the two cavity fields while the auxiliary qubits  $\alpha$  and  $\beta$  are encoded in the  $|g\rangle, |e\rangle$  states of the two atoms. To be more specific, in what follows we can consider the two circular levels of rubidium atoms with principal quantum numbers  $\mu_e = 50$  (for the excited state  $|e\rangle$ ) and  $\mu_g = 49$  (for the ground state  $|g\rangle$ ) [44]. We neglect here the hyperfine structure of the chosen atomic levels which is hardly resolved in a realistic experiment [14]. The  $|e\rangle \leftrightarrow |g\rangle$  transition frequency is  $\nu_0 \simeq 54$  GHz (wavelength  $\lambda_0 \simeq 6$  mm). The radiative lifetime  $\tau_{atom}$  of these circular levels of the Rydberg spectrum of rubidium is about 30 msec [13] while, for  $Q \simeq 10^8$  and a cavity mode frequency  $\nu$  nearly resonant with  $\nu_0$ , the field energy damping time  $\tau_{field}$  ranges from 1 up to 30 msec [13]. Each cavity can be cooled by a refrigerator in order to avoid blackbody radiation. The atom-cavity field coupling factor, measured by the Rabi frequency  $\Omega$ , can be as large as  $10^5$  sec $^{-1}$  so that we can write  $1/\Omega \ll \tau_{field}, \tau_{atom}$ . This means that it is possible to observe coherent interaction between atom and cavity field mode before the occurrence of dissipative or decohering effects due to the relaxation of the cavity fields

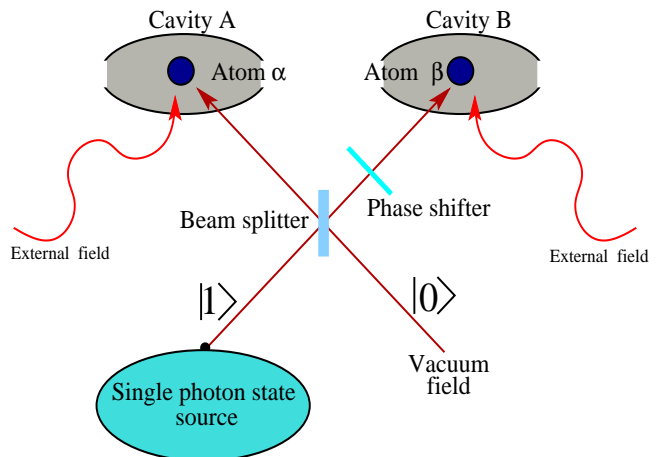


FIG. 2: Sketch of the experimental set-up for a non-local quantum computer implemented in a CQED system. The atoms are trapped inside each cavity (atomic traps are not shown). The external classical fields allow the manipulation of the atomic states. We show a brief sketch of the apparatus we intend to use to create entanglement between the atoms.

or the decaying of the atoms. Thus, in the following, we neglect any decoherence mechanism and the dynamics of the whole atom-cavity mode system is governed by a Schrödinger equation [13, 15]. In such set-up the interaction of each two-level atom with a single mode of electromagnetic field is well described by the Jaynes-Cummings Hamiltonian model [16]:

$$H_{JC} = \frac{1}{2}\hbar\omega_0\sigma_z + \hbar\omega\left(a^\dagger a + \frac{1}{2}\right) + \hbar\Omega\left(a^\dagger\sigma_- + a\sigma_+\right) \quad (5)$$

where  $a^\dagger$  and  $a$  are the bosonic operators and  $\omega = 2\pi\nu$  the angular frequency of the field mode;  $\sigma_+ = \sigma_-^\dagger = |e\rangle\langle g|$ ,  $\omega_0 = 2\pi\nu_0$  and  $\sigma_z = (|e\rangle\langle e| - |g\rangle\langle g|)$  are the raising atomic operator, the  $|e\rangle \leftrightarrow |g\rangle$  angular frequency and the third Pauli operator respectively.

In the Hilbert space  $\mathcal{H} = \mathcal{H}_{atom} \otimes \mathcal{H}_{field}$ , the state  $|g, 0\rangle$  is an eigenstate of  $H_{JC}$  with energy  $E_{g,0} = -\hbar\delta/2$ , where  $\delta = \omega_0 - \omega$  is the atom-cavity mode detuning. Apart from  $|g, 0\rangle$ , the energy spectrum of the system is divided into manifolds, essentially labeled by the number of photons in the cavity field  $n$ , each formed by the unperturbed states  $\{|e, n\rangle, |g, n+1\rangle\}$  (for  $n \geq 0$ ). The diagonalization of  $H_{JC}$ , in each manifold with an assigned value of  $n$ , leads to the well-known dressed states:

$$\begin{cases} |\mathcal{V}_+^n\rangle = \cos\varphi_n |e, n\rangle + \sin\varphi_n |g, n+1\rangle \\ |\mathcal{V}_-^n\rangle = -\sin\varphi_n |e, n\rangle + \cos\varphi_n |g, n+1\rangle \end{cases} \quad (6)$$

where  $\tan(2\varphi_n) = (2\Omega\sqrt{n+1})/\delta$  [13]. The corresponding eigenenergies are:

$$E_{\pm}^{(n)} = \hbar\omega(n+1) \pm \hbar\sqrt{(\delta/2)^2 + \Omega^2(n+1)}. \quad (7)$$

By suitably varying the detuning  $\delta$  it is possible to couple - decouple the atom and the cavity mode and to coherently mix the bare states which in the following will be

used to encode quantum information. Assume for instance that at  $t = 0$  the state of the system is  $|g, n+1\rangle$  and that we suddenly switch  $\delta = 0$ : the state will undergo a Rabi flipping as

$$|\psi(t)\rangle = \cos(\Omega\sqrt{n+1}t) |g, n+1\rangle - i \sin(\Omega\sqrt{n+1}t) |e, n\rangle. \quad (8)$$

On the contrary, in the *dispersive regime* defined by  $\Omega\sqrt{n+1} \ll \delta$  the atom is decoupled from the cavity and there is no coherent exchange of quantum excitations between atom and field and quantum Rabi oscillations are absent.

We conclude this section by describing how an external classical field couples with the dressed states. Suppose that an external pulse, sufficiently intense to be considered a classical field, is switched on the atom inside the cavity. In [13], this external source is a high-frequency Schottky diode, able to provide a quasi-monochromatic field tunable between 40 GHz and 300 GHz (see [13] and references within). The shape of the field is mathematically described by a smooth function. In electric dipole approximation, the Hamiltonian describing the atom-external pulse interaction can be written as

$$H_S(t) = \hbar g(t) \{\sigma_+ + \sigma_-\} \quad (9)$$

where  $g(t)$  is a function that includes the shape of the pulse and the atom-field coupling coefficient [15]. It is straightforward to rewrite (9) in terms of dressed states. One important point is that the external field couples dressed states that belong to adjacent manifolds only:  $H_S(t)$  has non-null matrix elements just for dressed states that satisfy  $\Delta n = \pm 1$ . This fact allows us to extract a simple  $4 \times 4$  block, relative to the subspace spanned by  $\{|\mathcal{V}_+^{n-1}\rangle, |\mathcal{V}_-^{n-1}\rangle, |\mathcal{V}_+^n\rangle, |\mathcal{V}_-^n\rangle\}$ , from the matrix representing  $H_S(t)$ :

$$H_S^{(n)} = \hbar g(t) \begin{pmatrix} 0 & 0 & \cos\varphi_n \sin\varphi_{n-1} & -\sin\varphi_n \sin\varphi_{n-1} \\ 0 & 0 & \cos\varphi_n \cos\varphi_{n-1} & -\sin\varphi_n \cos\varphi_{n-1} \\ \cos\varphi_n \sin\varphi_{n-1} & \cos\varphi_n \cos\varphi_{n-1} & 0 & 0 \\ -\sin\varphi_n \sin\varphi_{n-1} & -\sin\varphi_n \cos\varphi_{n-1} & 0 & 0 \end{pmatrix} \quad (10)$$

$H_S(t)$  sums to Hamiltonian  $H_{JC}$ , which is diagonal in the dressed states basis, and the Schrödinger equation for the time evolution of an arbitrary state  $|\xi\rangle = a(t)|\mathcal{V}_+^{n-1}\rangle + b(t)|\mathcal{V}_-^{n-1}\rangle + c(t)|\mathcal{V}_+^n\rangle + d(t)|\mathcal{V}_-^n\rangle$  leads to a system of coupled differential equations with time-dependent coefficients that, in general, is not easy to solve. We will see that, under precise conditions on  $\delta$  and on the pulse properties, some important approximations could be performed on these equations. We will show how the interaction regimes described briefly above

can be used for the realization of a non-local CNOT.

#### IV. NON-LOCAL CNOT

In this section we describe how to implement, in our CQED systems, the optimal protocol for a non-local CNOT operation. In our scheme, the control qubit of the gate is encoded in the zero and one photon states of a mode of the electromagnetic field sustained by cavity

A. Similarly, cavity  $B$  sustains the field mode representing the target qubit. The initial state of modes  $A$  and  $B$  will be prepared in

$$(a|1\rangle + b|0\rangle)_A \otimes (c|1\rangle + d|0\rangle)_B. \quad (11)$$

We want to prove that the experimental scheme we propose is able to change this state into

$$a|1\rangle_A \otimes (c|0\rangle + d|1\rangle)_B + b|0\rangle_A \otimes (c|1\rangle + d|0\rangle)_B. \quad (12)$$

We give here the entire list of operations to implement the non-local CNOT, leaving to the following subsections a detailed treatment of each one.

1. **Trapping:** the two-levels atoms  $\alpha$  and  $\beta$  should be trapped inside the spatially separated microwave cavities.
2. **Setting of the initial state of the register:** using  $\pi$ -Rabi pulses, we prepare the initial state of modes  $A$  and  $B$  and of atoms  $\alpha$  and  $\beta$ .
3. **Setting of the ebit: preparation of an entangled atomic state.** We set entanglement in the joint state of the trapped atoms letting  $\alpha$  and  $\beta$  interact directly with a previously prepared entangled single-photon state. Even if the expression “single-photon state” seems to be more appropriate for the visible range of frequency, it will however be used, in what follows, for millimeter-wave radiation too. In this case, we simply want to indicate the state of a field with a single quantum of excitation whose energy, measured in frequency units, falls into the microwave region of the radiation spectrum.
4. **Local CNOT cavity  $A \rightarrow$  atom  $\alpha$  and measurement of the state of atom  $\alpha$ :** the gate is implemented driving, by an external laser pulse, a transition between two specific levels of the dressed spectrum of atom  $\alpha$ . The measurement of the atomic state is made inducing cyclic transitions to a third level and detecting the subsequent signal with a *millimeter-wave receiver*.
5. **Local CNOT atom  $\beta \rightarrow$  cavity  $B$ :** we realize this transformation with a two-photon transition between two particular dressed states of atom  $\beta$  and using a CNOT cavity  $B \rightarrow$  atom  $\beta$ .
6. **Hadamard transform on atom  $\beta$ :** using  $\pi/2$ -pulses we create linear combinations, with equal weights, of states  $|e\rangle_\beta$  and  $|g\rangle_\beta$ .

#### Step 1: trapping of the atoms inside the cavities

We need to trap each atom inside its respective cavity for a time sufficient to perform every step required by the protocol for a non-local CNOT. Furthermore, the

trapping volume should be as small as possible to pledge a strong atom-cavity field coupling.

These features, long trapping time and small volumes, are usually typical of a Far-Off-Resonance-Trap (FORT) [17]. This is realized by a very focused laser beam of frequency tuned below the atomic resonance [18]. In these conditions the dipole force confines the atom in a potential well. Cooling is obtained by means of the scattering force furnished by optical molasses [19]. This mixture of dipole and scattering force characterizes this trap as an hybrid one [18].

Using a FORT to confine neutral atoms is a common practice in the optical domain and allows to reach trapping time of a hundred of seconds, in a high vacuum environment [20]. Recently, trapping a single atom in a cavity using Magneto-Optic-Traps (MOT) [18] and a FORT has been proved [21]. The trapping times can be improved if a cryostat is used in addition [20].

In the microwave range of frequency, on the other hand, the work by Spreeuw *et al.* [22] proved experimentally the possibility to combine an MOT and a microwave cavity. A MOT and a system of optical molasses are there used to load a microwave cavity with an ensemble of alkali atoms. The minimum of the MOT trapping potential is located in the center of the cavity and the temperature of the atoms is kept, by the optical molasses, between 3 and 5  $\mu\text{K}$  [22]. Even if the experiment has been performed with a large number of atoms, it however represents an insight into the realistic mixing of microwave cavities and conventional optical trapping techniques (furthermore, an alternative trapping scheme that uses microwaves and an external static magnetic field as a trap for neutral atoms has been addressed both theoretically and experimentally [22, 23]).

The recent and fast improvement of the technique of atomic trapping and the increase in the control of microwave resonators allow to consider the *scenario* we propose as not far from practical realization. Particularly promising, in this context, are the recently developed techniques for the realization of arrays of single, selectively addressable dipole traps that, because of their very reduced dimensions, could be implanted directly inside the cavity without spoiling its  $Q$  quality factor too much [24].

#### Step 2: preparation of the distributed register

The value of the detuning  $\delta = 0$  can be controlled by means of the so-called *Stark switching technique* that uses an external electric field applied to the atom [25]. If the atom has no permanent electric dipole moment, the Stark effect will be quadratic in the electric field amplitude [26]. This induces a relative shift on the atom’s energy spectrum between states  $|e\rangle$  and  $|g\rangle$  so that the transition frequency changes from  $\omega_0$  to another frequency  $\omega'_0$ . The cavity mode frequency, on the other hand, will remain unchanged. The width and the amplitude of the Stark

field pulses can be controlled with high accuracy, allowing a very precise control of the atomic level separation [25]. Choosing the amplitude of the Stark field in such a way that  $\omega'_0 - \omega \gg 2\Omega\sqrt{n+1}$ , we are able to decouple the atom from the cavity field. In such dispersive regime it is possible to change the atomic state without modifying the cavity mode population by means of an external electromagnetic field, resonant with the new transition frequency  $\omega'_0$ . It is therefore possible to prepare qubit  $\alpha$  ( $\beta$ ) in  $\tilde{a}|e\rangle_\alpha + \tilde{b}|g\rangle_\alpha$  ( $\tilde{c}|e\rangle_\beta + \tilde{d}|g\rangle_\beta$ ).

The coefficients of these linear combinations can be set fixing the width of each pulse. If the cavities are initially prepared in  $|0\rangle_A \otimes |0\rangle_B$  (a procedure to obtain such initial states for the cavities is suggested in ref. [27]) the joint system  $A+B+\alpha+\beta$  will be described by the tensor product state:

$$|\varphi\rangle = (\tilde{a}|e\rangle + \tilde{b}|g\rangle)_\alpha \otimes (\tilde{c}|e\rangle + \tilde{d}|g\rangle)_\beta \otimes |00\rangle_{AB} \quad (13)$$

By switching the detuning to its value  $\delta = 0$  a coherent exchange of quantum excitations between each atom and the relative cavity field takes place. If we leave them to interact resonantly for a time  $t = \pi/(2\Omega)$  ( $\pi$ -Rabi pulse) we obtain a complete inversion between states  $|0e\rangle$  and  $|1g\rangle$  for each atom+cavity system (see section III). State  $|0g\rangle$ , on the contrary, being an eigenstate of  $H_{JC}$ , is not modified by the resonant interaction. The operations described above, based on the atom-cavity mode local resonant interaction, can be realized with high accuracy [13]. The effect of the  $\pi$ -pulses is to change  $|\varphi\rangle_{\alpha\beta AB}$  into:

$$\begin{aligned} &|g\rangle_\alpha \otimes |g\rangle_\beta \otimes |\varphi_{in}\rangle_A \otimes |\varphi_{in}\rangle_B = \\ &|g\rangle_\alpha \otimes |g\rangle_\beta \otimes (a|1\rangle + b|0\rangle)_A \otimes (c|1\rangle + d|0\rangle)_B. \end{aligned} \quad (14)$$

We have created initial states of the cavity modes which are coherent superpositions of Fock states with zero and one photon. The state for atoms  $\alpha+\beta$  is, at this moment,  $|g\rangle_\alpha \otimes |g\rangle_\beta$ : we will further manipulate it, in the next step of our scheme, to prepare the required ebit.

### Step 3: preparation of the atomic ebit

In the scheme we propose, the trapped atoms  $\alpha$  and  $\beta$  encode an ebit, the quantum resource to the non-local implementation of the  $\text{CNOT}_{AB}$ . The state could be prepared by letting the atoms interact with a pair of external microwave fields previously prepared in the maximally entangled state:

$$|\psi_+\rangle = \frac{1}{\sqrt{2}}(|01\rangle + |10\rangle). \quad (15)$$

A possible way to get this state of radiation is using a *photon gun*, a device which is able to generate single photon wave packets on demand, in a nearly deterministic way. There are many proposals for single-photon sources: semiconductor quantum dots, one-photon emission by isolated molecules, stimulated adiabatic rapid

passages of neutral atoms strongly coupled to a resonator or strongly attenuated beams [28]. In this attenuation scheme, a pulsed laser field is simply attenuated with density filters until there is on average a fraction of a photon per pulse [29]. The technique should be feasible and can be accomplished even at the range of wavelengths relevant to our set-up. The pulse can then be sent to a 50 : 50 beam splitter (BS), whose second input is the vacuum field. The effect of the BS is to mix the two input fields. By properly setting the relative phase between the output fields by means of a phase shifter, the joint output state is the maximally entangled state written in Eq. (15) [30].

Another possible scheme for the generation of single-photon states of radiation is based on the *no-pass* scheme of Hong and Mandel [31]: via a process of Spontaneous-Parametric-Down-Conversion (SPDC) [32], a signal and an idler photon are simultaneously generated (within an uncertainty of 100 psec [31]). The two emitted photons are entangled in momentum [33] and if one of them is detected, at some position and within a temporal window  $T$ , then we are sure that there is a conjugate idler photon, in the corresponding position and inside the same window. Thus, if by means of a photon-counting apparatus a single photon is detected in the signal, the idler is instantaneously prepared in a single-photon state. Furthermore, the experiment performed by Hong and Mandel has shown that the probability that more than just one signal photon is generated by the SPDC is negligible with respect to that of a single-photon generation. This procedure is thus able to create, with a good accuracy, a single-photon state of radiation that can, then, be sent to the same BS described above in order to realize state (15).

The next step we have to perform to get an entangled atomic state is the direct interaction of the trapped atoms  $\alpha$  and  $\beta$  with  $|\psi_+\rangle$ . The entangled photons we prepared are sent to the atoms (via suitable designed waveguides directly coupled to the cavities  $A$  and  $B$ , for example). In each cavity-atom subsystem, a dispersive regime of interaction should be set, so that the atom dynamics is decoupled from that of the cavity.

If the spectrum of each light pulse is sufficiently narrow and centered at a frequency resonant to the atomic transition  $|g\rangle \leftrightarrow |e\rangle$ , it is possible to show that setting the interaction time in order to realize a  $\pi$ -pulse, the following transformation can be realized:

$$|g\rangle_\alpha \otimes |g\rangle_\beta \rightarrow \frac{1}{\sqrt{2}}(|eg\rangle + |ge\rangle)_{\alpha\beta}. \quad (16)$$

However, these two techniques are not immune to problems. In the case of the attenuated beam, at a so low intensity level, it is not possible to be sure there being a photon. There is always a possibility to get an empty pulse or a two-photon one. In the latter case, even if the procedure described is able to generate atomic entanglement, the state consequently obtained is not of the form we need. Even more, as we have seen, a precise control

of the area of the pulse is required in order to accomplish exactly the required atomic evolution.

On the other hand, the Hong and Mandel scheme presents some difficulties for the microwave range of frequencies because it is based on a SPDC process. The generation efficiency of the couple of conjugate photons, in a down-conversion process, is very low (a rough but, for our purposes, sufficient semiclassical approach to the theory of SPDC shows that it is directly proportional to the fourth power of the pump beam frequency  $\omega_p^4$ ). Typically, optical frequency beams are used as pumps for SPDC (Ultra-Violet in [31]) and this gives a rate of generation of down converted photons of the order of  $10^{-10} \text{ sec}^{-1}$ . For microwave frequencies the rate of down conversion is dramatically smaller than this value and makes the scheme useless as a photon gun. Even more, technical difficulties, in the microwave case, have to be managed. The crystal used for the generation of signal and idler, for example, has to be almost transparent to the frequency of both the pump and the down converted fields. Finding an appropriate candidate for a pump that falls in the microwave range is a non trivial task.

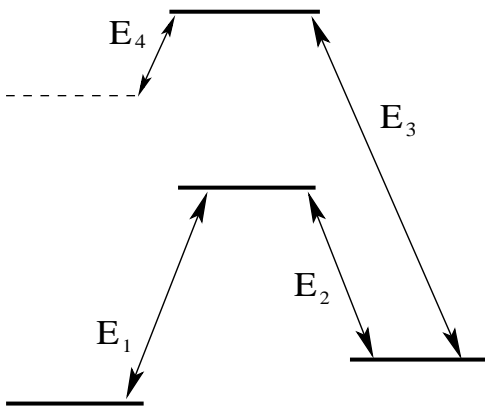


FIG. 3: Scheme of the atomic levels for the generation of a microwave field by means of a four-wave-mixing process. If  $E_2$  is slowly turned off while  $E_1$  enters in an optically thick medium, the quantum information carried by  $E_1$  is stored in the coherences established between the ground, metastable states of the atomic model. If the *reading* field  $E_3$  is then turned on, for properly chosen values of its frequency, a fourth field, in the microwave range of frequencies, could be generated.

A deterministic source of one-photon states has been theoretically proposed and, recently, experimentally demonstrated in the microwave range of frequencies [35]: it is based on the interaction of a beam of Rydberg atoms with a field mode of a very high- $Q$  microwave cavity (in the experiment  $Q \sim 10^{10}$ ). Unfortunately, the enormous  $Q$  value of the cavity used in [35] prevents significant leakage of the field from the cavity itself and, thus, the scheme does not produce any exploitable output beam.

The recently developed techniques to store the quantum state of a field in a macroscopic atomic ensemble that exhibits electromagnetically-induced-transparency (EIT) [36] could represent a possible solution to the prob-

lem represented by the production of a microwave single photon state. Assume that the preparation of a one-photon state of an optical pulse, as experimentally done in [31], is followed by a *storage* step in an optically thick medium made by three-level atoms in a  $\Lambda$  configuration [36]. For the notation of the following discussion we refer to Fig. 3. If the field  $E_2$ , with wavevector  $\mathbf{k}_2$ , is slowly turned off while  $E_1$  (wavevector  $\mathbf{k}_1$ ) interacts with the atomic medium, the quantum information about the amplitude, shape and phase of the latter is transferred to the coherences established between the two ground (metastable) states of the atomic model. To recover the information so stored, a *reading* pulse is necessary. If a field  $E_3$  is shined on the ensemble, the new electromagnetic field  $E_4$ , with a wavevector  $\mathbf{k}_4$  that satisfies the *phase matching condition*  $\mathbf{k}_1 + \mathbf{k}_2 = \mathbf{k}_3 + \mathbf{k}_4$ , is generated by means of a process of forward four-wave-mixing [37]. Properly choosing the values for the angular frequencies  $\omega_j = ck_j$  ( $j = 1, 3$ ), the generated field can fall in the microwave range [38].

#### Step 4: local CNOT $A \rightarrow \alpha$ and measurement of the state of atom $\alpha$

The theoretical protocol requires a CNOT having cavity  $A$  as control and atom  $\alpha$  as target. Since this unitary operation involves just one cavity and the respective trapped atom, we refer to  $\text{CNOT}_{A\alpha}$  as a local transformation to distinguish it from the non-local one we want to perform between cavity  $A$  and cavity  $B$ . The computational basis for the  $\text{CNOT}_{A\alpha}$  is  $\{|0g\rangle, |0e\rangle, |1g\rangle, |1e\rangle\}_{A\alpha}$  and the set of transformations we should realize is:

$$\begin{aligned} |0g\rangle_{A\alpha} &\rightarrow |0g\rangle_{A\alpha} & |0e\rangle_{A\alpha} &\rightarrow |0e\rangle_{A\alpha} \\ |1g\rangle_{A\alpha} &\rightarrow |1e\rangle_{A\alpha} & |1e\rangle_{A\alpha} &\rightarrow |1g\rangle_{A\alpha}. \end{aligned} \quad (17)$$

According to this set of transformations, the state prepared during Step 3:

$$|\chi\rangle = \frac{1}{\sqrt{2}}(|eg\rangle + |ge\rangle)_{\alpha\beta} (a|1\rangle + b|0\rangle)_A (c|1\rangle + d|0\rangle)_B \quad (18)$$

has to be changed into:

$$\begin{aligned} \text{CNOT}_{A\alpha} |\chi\rangle &= \frac{1}{\sqrt{2}} \{a|1\rangle_A (|gg\rangle + |ee\rangle)_{\alpha\beta} \\ &\quad + b|0\rangle_A (|eg\rangle + |ge\rangle)_{\alpha\beta}\} (c|1\rangle + d|0\rangle)_B. \end{aligned} \quad (19)$$

Expressions (17) and (19) show that, while the atomic state can modify its state, the cavity mode population does not change: this means that a resonant coupling between  $A$  and  $\alpha$  can not be used to implement the gate. Resonant Rabi oscillations, indeed, preserves the total number of excitations while the last two transformations in (17) do not. We need a dispersive atom-cavity field interaction; the atomic state will be manipulated by an

external electromagnetic field. If the external field is resonant with a field mode sustained by the cavity but different from the relevant one used to codify the cavity qubit, it can enter the resonator without feeding this latter mode (for example we can choose two orthogonally polarized field modes: in [13] two orthogonally polarized transverse modes, with a spacing in frequency of 70 kHz, sustained by a millimeter-wave cavity are considered). Using the Stark switching technique, the trapped atom can then interact with the external field, being decoupled with respect to the relevant cavity mode, for a controlled amount of time.

The Stark field can be set to change the separation between levels  $|e\rangle_\alpha$  and  $|g\rangle_\alpha$  and to obtain a value of  $\delta$  that allows to write  $\Omega \ll \delta$ . In such a condition, from Eq. (6), it results that  $|\mathcal{V}_+^n\rangle \simeq |n, e\rangle$ ,  $|\mathcal{V}_-^n\rangle \simeq |n+1, g\rangle$ . Therefore, if using an appropriate external pulse we can induce a complete inversion of population between  $|\mathcal{V}_+^1\rangle$  and  $|\mathcal{V}_-^0\rangle$ , we mutually exchange  $|1e\rangle$  and  $|1g\rangle$  without involving the other dressed states,  $|\mathcal{V}_+^0\rangle \simeq |0e\rangle$  and  $|\mathcal{V}_-^1\rangle \simeq |2g\rangle$ . The only approximative identification of the bare basis elements with the corresponding dressed states in the limit of large detuning has only a very small effect on the fidelity of the gate, as we show below.

Since we want the interaction of atom  $\alpha$  with an external pulse, we use results obtained in III: the dressed manifolds involved in the transition  $|\mathcal{V}_+^1\rangle \leftrightarrow |\mathcal{V}_-^0\rangle$  are those with  $n=0$  and  $n=1$  (therefore satisfying condition  $\Delta n = \pm 1$ ). We give explicit expression for  $H_S^{(1)}(t)$  expanding each matrix element in Taylor series, to second order in  $\Omega/\delta$ :

$$\frac{H_S^{(1)}}{\hbar} = g(t) \begin{pmatrix} 0 & 0 & \frac{\Omega}{\delta} & -\sqrt{2}\frac{\Omega^2}{\delta^2} \\ 0 & 0 & \left(1 - \frac{3}{2}\frac{\Omega^2}{\delta^2}\right) & -\sqrt{2}\frac{\Omega}{\delta} \\ \frac{\Omega}{\delta} & \left(1 - \frac{3}{2}\frac{\Omega^2}{\delta^2}\right) & 0 & 0 \\ -\sqrt{2}\frac{\Omega^2}{\delta^2} & -\sqrt{2}\frac{\Omega}{\delta} & 0 & 0 \end{pmatrix} \quad (20)$$

We deduce that if the experimental parameters are such that  $\Omega \ll \delta$ , the matrix elements belonging to the central  $2 \times 2$  block in  $H_S^{(1)}$  predominates over all the others. We choose  $g(t)$  so that  $g(t) = p(t) \cos(\omega_S t)$ , with  $p(t)$  a smooth function describing the envelope shape of the pulse shined on the trapped atom. We set  $\omega_S$  to be equal to the transition frequency for  $|\mathcal{V}_+^1\rangle \leftrightarrow |\mathcal{V}_-^0\rangle$ :

$$\omega_S = \frac{E_+^1 - E_-^0}{\hbar} \quad (21)$$

With a suitable choice of the pulse duration, the right inversion of population can be obtained. In particular, it has to be  $\int^t p(t') dt' = \pi$  (we refer to this case as to a  $\pi$  pulse). Any spurious phase factor can be adjusted by setting an appropriate phase in function  $g(t)$  or using appropriate Stark field and, in what follows, we do not care about it [15]. Achievable coupling strength for the atom-external field interaction as large as  $20\pi$  kHz and

interaction times of about  $50 \mu\text{sec}$  allow to get a complete  $\pi$  pulse.

The effect of a finite, non null, value of the ratio  $\Omega/\delta$  on the state that we instead obtain, can be seen if we propagate  $|\chi\rangle$  by means of the unitary operator that is generated by the Hermitian interaction Hamiltonian  $H_S^{(1)}(t)$ . We assume  $x = \Omega/\delta = 0.1$ , value that allows for the approximations discussed above and for the discrimination between the frequencies of the different transitions involved; retaining just the terms up to the second order in  $\Omega/\delta$ , we get an approximate expression for the evolved state of the system  $|\tilde{\chi}\rangle$ . This expression is useful in order to find the fidelity of the local CNOT operation we are performing.

The definition of the fidelity function, in this case, reads  $\mathcal{F} = |\langle \chi | \text{CNOT}_{A\alpha} | \tilde{\chi} \rangle|^2$  [7] and assuming for simplicity  $a = b = \frac{1}{\sqrt{2}}$ , it is possible to show that:

$$\mathcal{F}(x) = \frac{1}{4} \left\{ 1 + \sin \left[ \frac{\pi}{2} \left( 1 - \frac{3}{2} x^2 \right) \right] \right\}^2 + 0.003 x^2. \quad (22)$$

Notice that, as  $\Omega/\delta \rightarrow 0$ , the fidelity reaches  $\mathcal{F} = 1$ , which shows a perfect overlap between the state we need and the one we get manipulating the atomic qubit by an external field.

The state of the system at the end of Step 3 becomes:

$$\begin{aligned} & \frac{1}{\sqrt{2}} |g\rangle_\alpha \otimes (-ia |1g\rangle + b |0e\rangle)_{A\beta} \otimes |\varphi_{in}\rangle_B + \\ & \frac{1}{\sqrt{2}} |e\rangle_\alpha \otimes (-ia |1e\rangle + b |0g\rangle)_{A\beta} \otimes |\varphi_{in}\rangle_B. \end{aligned} \quad (23)$$

We now measure the state of atom  $\alpha$  on the bare eigenstate basis  $\{|e\rangle, |g\rangle\}_\alpha$ . We enlarge the Hilbert space of the atom introducing a third energy level,  $|m\rangle_\alpha$ , whose

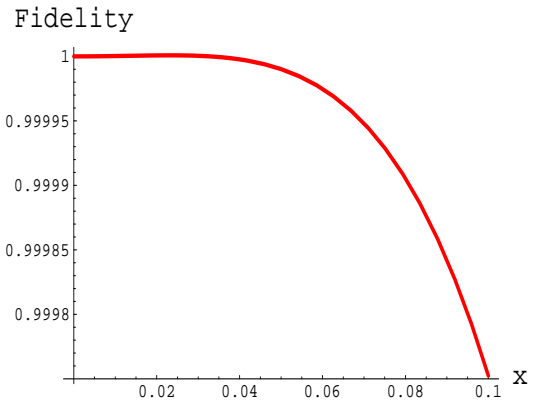


FIG. 4: Plot of the fidelity function  $\mathcal{F}$  of the local  $\text{CNOT}_{A\alpha}$  operation as a function of the ratio  $x = \Omega/\delta$  and for  $a = b = 1/\sqrt{2}$ . As it is shown, for values of  $x$  that range from 0 to 0.1, the gate can be performed with a very high accuracy. The high fidelity of the gate is maintained even for different choices of  $a$  and  $b$ .



parity is opposite to that of  $|e\rangle_\alpha$ . For example, we can take the Rydberg level with principal quantum number  $\mu_m = 51$ . In this case the  $|e\rangle_\alpha \leftrightarrow |m\rangle_\alpha$  frequency is about  $\nu_m \simeq 51.1$  GHz [13]. An external microwave field couples  $|e\rangle_\alpha$  to  $|m\rangle_\alpha$ . If the state of  $\alpha$  is  $|e\rangle_\alpha$ , the external field induces cyclic transitions between these states but, if atom  $\alpha$  is in  $|g\rangle_\alpha$ , because of the large frequency mismatch, we do not detect any signal. If  $|m\rangle_\alpha$  corresponds to a low angular quantum number, the emission time of the atom falls in the range of  $\mu\text{sec}$  [13, 39]. The radiation emitted by the cycling atom can be collected by a *millimeter – wave receiver* [39]. This is, essentially, a Schottky diode detector that mixes the signal to be measured with a local reference microwave field to perform a heterodyne measurement of the signal. The response time of the device is short enough not to represent a limitation for our purposes. This detection technique has been successfully used in the context of micromaser spectroscopy to directly infer the radiation of a millimeter-wave field inside a cavity [13, 39].

Depending on the state of atom  $\alpha$  at the end of the measurement process, system  $A + \beta + B$  is projected onto states which differ just for the state of atom  $\beta$ . In order to obtain the right final state at the end of the protocol for the non-local  $\text{CNOT}_{AB}$ , if the atomic state detection gives  $|g\rangle_\alpha$ , we should change nothing in subsystem  $B + \beta$ . If the output of the measurement is  $|e\rangle_\alpha$ , a **NOT** is required for qubit  $\beta$ .

To obtain it we essentially need the same kind of transformations we introduced in the last step:  $|1e\rangle_{B\beta} \rightarrow |1g\rangle_{B\beta}$  and  $|0g\rangle_{B\beta} \rightarrow |0e\rangle_{B\beta}$ . They can be realized by applying  $\pi$ -pulses for transitions between suitable dressed states of the atom  $\beta$  in a dispersive regime of interaction. In any case, with a fidelity that approaches 100%, the system  $A + \beta + B$  can be set in  $(-ia|1g\rangle + b|0e\rangle)_{A\beta} \otimes |\varphi_{in}\rangle_B$  apart from a global phase factor. For simplicity, in the following, we assume to have detected  $|g\rangle_\alpha$ .

### Step 5: local $\text{CNOT } \beta \rightarrow B$

The next step is the implementation of a local  $\text{CNOT}_{\beta B}$ . The atomic qubit  $\beta$  is now the control of the gate. To get the right final state for the non-local  $\text{CNOT}_{AB}$ , the set of transformations to realize is the following:

$$\begin{aligned} |g0\rangle_{\beta B} &\rightarrow |g1\rangle_{\beta B} & |g1\rangle_{\beta B} &\rightarrow |g0\rangle_{\beta B} \\ |e0\rangle_{\beta B} &\rightarrow |e0\rangle_{\beta B} & |e1\rangle_{\beta B} &\rightarrow |e1\rangle_{\beta B}. \end{aligned} \quad (24)$$

It is clear that, in (24), we have  $|g\rangle \equiv |1\rangle$  and  $|e\rangle \equiv |0\rangle$ . In this subsection we show how to realize these transformations using the two-photon transition  $|g0\rangle_{\beta B} \leftrightarrow |\mathcal{V}_+^1\rangle_{\beta B}$  and a  $\text{CNOT}_{\beta B}$ .

We need such a different strategy because an approach similar to that used for the  $\text{CNOT}_{A\alpha}$  will lead us to some inconsistencies. In effect, using the same logic scheme

used to implement the Step 4, a procedure to get transitions (24) could be the following. We induce a  $\pi$ -pulse between  $|g0\rangle_{\beta B}$  and  $|\mathcal{V}_-^0\rangle_{\beta B}$ . State  $|\mathcal{V}_-^0\rangle_{\beta B}$ , for  $\Omega \ll \delta$ , is in practice the bare state  $|g1\rangle_{\beta B}$  but, for the selection rules relative to electric dipole transitions [26], transition  $|g0\rangle_{\beta B} \leftrightarrow |g1\rangle_{\beta B}$  is strictly forbidden. Since  $|\mathcal{V}_-^0\rangle_{\beta B}$  holds a little contribution from  $|e0\rangle_{\beta B}$  [15], transition  $|\mathcal{V}_-^0\rangle_{\beta B} \leftrightarrow |g0\rangle_{\beta B}$  can be realized. Using the same procedure of previous sections we can obtain the matrix representation of the Hamiltonian  $H_S(t)$  for the interaction of the dressed atom  $\beta$  with the external pulse driving the required transition. On the ordered dressed basis  $\{|g0\rangle_{\beta B}, |\mathcal{V}_-^0\rangle_{\beta B}, |\mathcal{V}_+^0\rangle_{\beta B}\}$ , we have

$$H_S^{(0)}(t) = \hbar g(t) \begin{pmatrix} 0 & -\frac{\Omega}{\delta} \left(1 - \frac{1}{2} \frac{\Omega^2}{\delta^2}\right) \\ -\frac{\Omega}{\delta} & 0 & 0 \\ \left(1 - \frac{1}{2} \frac{\Omega^2}{\delta^2}\right) & 0 & 0 \end{pmatrix} \quad (25)$$

Here, the biggest matrix elements are those that connect  $|g0\rangle_{\beta B}$  to  $|\mathcal{V}_+^0\rangle_{\beta B}$  and vice versa. For  $\Omega \ll \delta$ ,  $|\mathcal{V}_+^0\rangle_{\beta B}$  is essentially identified with  $|e0\rangle_{\beta B}$  [45]. On the contrary, the probability of a transition  $|g0\rangle_{\beta B} \leftrightarrow |\mathcal{V}_-^0\rangle_{\beta B}$  is directly proportional to  $\Omega/\delta$ . However, since we want  $\Omega \ll \delta$ , we need a different procedure.

We now proceed mapping the  $\text{CNOT}_{\beta B}$  into a sequence of three operations: two **SWAP** and a  $\text{CNOT}_{B\beta}$  (Fig. 5).

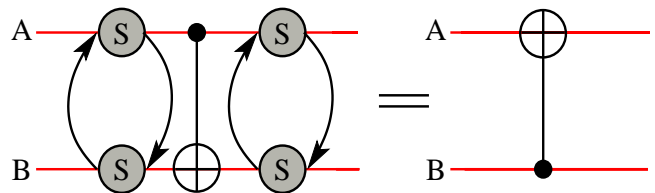


FIG. 5: A  $\text{CNOT}_{BA}$  gate can be simulated using the sequence of operations  $(\text{SWAP})(\text{CNOT}_{AB})(\text{SWAP})$ .

It is straightforward to prove that the sequence  $(\text{SWAP})(\text{CNOT}_{AB})(\text{SWAP})$  is equivalent to  $\text{CNOT}_{BA}$ . Since we have already seen an efficient way to implement a **CNOT** for the cavity qubit as control and the atomic one as target, we just pass to describe a possible procedure to accomplish a **SWAP** operation in a CQED system.

By the action of the **SWAP** gate, a transition occurs between  $|g0\rangle_{\beta B}$  and  $|e1\rangle_{\beta B}$ . For an external Stark field satisfying  $\Omega \ll \delta$ , the dressed state  $|\mathcal{V}_+^1\rangle_{\beta B}$  is about equal to  $|1e\rangle_{\beta B}$  as it can be deduced from Eq. (6). Inducing  $|\mathcal{V}_+^1\rangle_{\beta B} \leftrightarrow |0g\rangle_{\beta B}$  we can get what we want. Nevertheless, these dressed states belong to dressed manifolds which differ for two quantum excitations and that cannot be connected by a single photon transition. This means that we should go to the second order in the coupling coefficient, realizing a two-photon transition. We



choose it to be degenerate: this means that the photons involved in this second order process have the same energy  $\hbar\omega_L = \frac{1}{2}(E_+^{(1)} - E_{0g})$ , where the external field has frequency  $\omega_L$  [40].

The second order transition  $|\mathcal{V}_+^1\rangle_{B\beta} \leftrightarrow |0g\rangle_{B\beta}$  occurs via virtual transitions toward the intermediary states  $|\mathcal{V}_\pm^0\rangle_{B\beta}$ . In effect, because of the structure of the energy spectrum of the dressed atom, these states have energies which are very close to the middle energy between  $|0g\rangle_{B\beta}$  and  $|\mathcal{V}_+^1\rangle_{B\beta}$ . However, the transitions are not resonant, so that the probability that the system can accomplish an effective transition to  $|\mathcal{V}_\pm^0\rangle_{B\beta}$  is negligible. This qualifies  $|\mathcal{V}_\pm^0\rangle_{B\beta}$  as virtual states.

We model the external field as a linearly polarized pulse of Gaussian envelope:

$$E(t) = \mathcal{E}_0 e^{-\frac{t^2}{\tau^2}} \cos(\omega_L t). \quad (26)$$

The electric dipole interaction gives rise to the following interaction Hamiltonian:

$$H_L(t) = \hbar\Sigma_0 \left\{ e^{-\frac{t^2}{\tau^2} + i\omega_L t} |g\rangle\langle e| + h.c. \right\} \quad (27)$$

where  $\Sigma_0$  is the atom-field coupling coefficient and RWA has been used. The probability amplitude that the system, initially in  $|0g\rangle_{B\beta}$ , is found at time  $t$  in  $|\mathcal{V}_+^1\rangle_{B\beta}$  can be calculated using the following expression, directly derived from a second-order perturbation theory [41, 42]:

$$\begin{aligned} & \frac{1}{\hbar^2} \sum_{j=-,+} \left( \int_{-\infty}^t dt'' \langle \mathcal{V}_+^1 | H_L(t'') | \mathcal{V}_j^0 \rangle e^{\frac{i}{\hbar}(E_+^{(1)} - E_j^{(0)})t''} \times \right. \\ & \left. \times \int_{-\infty}^{t''} dt' \langle \mathcal{V}_j^0 | H_L(t') | 0g \rangle e^{\frac{i}{\hbar}(E_j^{(0)} - E_{0g})t'} \right) \end{aligned} \quad (28)$$

(with  $t'' > t'$ ). Explicit evaluation of this expression, with numerical values  $\Omega \approx 10^5$  Hz,  $\delta \approx 1$  MHz,  $\tau \approx 20$   $\mu$ sec,  $\Sigma_0 \approx 10^5$  Hz and for  $t = 3\tau$  leads to a transition probability equal to 0.47. The value of  $\delta$  satisfies the condition  $\delta \ll \omega, \omega_0$  because, for a millimeter-wave cavity, the value of  $\omega$  falls in the range from 10 to 100 GHz while a typical value for  $\omega_0$ , for values of the principal quantum number  $\mu \simeq 50$ , is 50 GHz [13]. Having  $\Sigma_0 \simeq \Omega_0$  ensures the observability of multiphotons transitions.

Since the explicit calculation for the  $|1e\rangle_{B\beta} \rightarrow |0g\rangle_{B\beta}$  case leads, with the same numerical values of the previous case, to the same probability of transition, our map of a  $\text{CNOT}_{\beta B}$  is valid for each initial state of the system  $\beta + B$ . Ideally, we are able to implement a  $\text{CNOT}_{\beta B}$  using just SWAP operations and  $\text{CNOT}_{\text{cavity-atom}}$ . In order to evaluate the fidelity of the local  $\text{CNOT}_{\beta B}$ , we have to perform essentially the same kind of calculation described in Step 4 for the case of the local  $\text{CNOT}_{A\alpha}$  gate. We found that, at the end of the operations, the state of the system  $A + B + \beta$  is projected onto

$$ia |g\rangle_\beta \otimes |1\rangle_A \otimes \{\text{NOT} |\varphi_{in}\rangle_B\} + b |0\rangle_A \otimes |e\rangle_\beta \otimes |\varphi_{in}\rangle_B \quad (29)$$

with a fidelity 0.54, for  $c = d = \frac{1}{\sqrt{2}}$  and after an average over all the possible initial configurations of the system  $B + \beta$ . This low value of the fidelity of the gate is essentially due to the non ideality of the two-photon transition and represents the major theoretical limitation to the efficiency of the proposed implementation.

### Step 6: Hadamard transform on atom $\beta$

We now need a Hadamard transform on qubit  $\beta$ . This can be realized, in a CQED system, recurring again to a dispersive regime of atom-cavity field interaction. In effect, setting a very large detuning (leaving the eigenstates of the atom  $\beta$  almost bare) and shining a driving external pulse on  $\beta$  for a time such that a  $\pi/2$ -pulse is realized between  $|ej\rangle$  and  $|gj\rangle$  ( $j = 0, 1$ ), we just obtain the following transitions:

$$\begin{aligned} |gj\rangle & \rightarrow \frac{1}{\sqrt{2}} \{|gj\rangle - i|ej\rangle\} \\ |ej\rangle & \rightarrow \frac{1}{\sqrt{2}} \{|ej\rangle - i|gj\rangle\}. \end{aligned} \quad (30)$$

We have, in practice, a Hadamard transform generalized by a relative phase factor that is not a problem for our scheme: using relations (30) in the state obtained at the end of Step 5, we have

$$\begin{aligned} & \frac{i}{\sqrt{2}} |g\rangle_\beta \otimes \{a|1\rangle \otimes (\text{NOT} |\varphi_{in}\rangle) - b|0\rangle \otimes |\varphi_{in}\rangle\}_{AB} + \\ & \frac{1}{\sqrt{2}} |e\rangle_\beta \otimes \{a|1\rangle \otimes (\text{NOT} |\varphi_{in}\rangle) + b|0\rangle \otimes |\varphi_{in}\rangle\}_{AB}. \end{aligned} \quad (31)$$

If the measurement outcome of the atom  $\beta$  is  $|e\rangle_\beta$ , system  $A + B$  is projected onto a state that shows the action of the  $\text{CNOT}_{AB}$  gate. An ulterior manipulation is required if the measurement outcome is  $|g\rangle_\beta$ . In this case, if we want to correct the  $-1$  relative phase factor that appears in the  $A + B$  state we just perform a  $2\pi$  resonant Rabi pulse in the subsystem  $A + \alpha$  (we remind that our measurement process is a non demolition one and that atom  $\alpha$  can always be forced to occupy state  $|g\rangle_\alpha$ , as we assumed all along our discussion).

This closes the scheme for a non-local  $\text{CNOT}$  between two spatially separated cavity modes.

## V. NON-LOCAL $\pi$ - CQPG

In this section we will describe a procedure for the physical implementation of a non-local controlled quantum phase gate with  $\phi = \pi$ . This is a very important task to accomplish because the set of quantum gates that comprehends controlled quantum phase gate and single qubit rotations is adequate for quantum computation. Our goal is to show that the experimental set-up proposed in this paper is sufficiently flexible to permit, with

slight modifications operated in Step 5 of the previous protocol, its feasible realization. As before, the computational register is formed by the two spatially separated cavity modes  $A$  and  $B$  while the atoms  $\alpha$  and  $\beta$  encode two ancillary qubits whose joint state constitutes an ebit.

We assume that the initial state for system  $A + B$  has been prepared as in Eq. (11). Moreover, we assume to have a maximally entangled atomic ebit. We want to show how to transform state  $|\varphi_{in}\rangle_A \otimes |\varphi_{in}\rangle_B$  into

$$ac|11\rangle_{AB} + ad|10\rangle_{AB} + bc|01\rangle_{AB} - bd|00\rangle_{AB}. \quad (32)$$

The experimental scheme for the non-local  $\pi$ -CQPG is identical until Step 4 to that for the non-local CNOT $_{AB}$ . This means that, at the end of Step 4, having performed the local CNOT $_{\alpha\alpha}$  and measured the state of atom  $\alpha$ , the state of system  $A + B + \beta$  is projected onto

$$(-iac|1g1\rangle - iad|1g0\rangle + bc|0e1\rangle + bd|0e0\rangle)_{A\beta B} \quad (33)$$

while atom  $\alpha$  is assumed to be in  $|g\rangle_\alpha$ .

We modify the previous scheme replacing Step 5 with the following to perform a  $\pi$ -CQPG on system  $\beta + B$ . We adopt the following map of the CQPG:

$$\begin{aligned} |e0\rangle &\rightarrow |e0\rangle & |e1\rangle &\rightarrow -|e1\rangle \\ |g0\rangle &\rightarrow |g0\rangle & |g1\rangle &\rightarrow |g1\rangle. \end{aligned} \quad (34)$$

This set of transformation is obtained by extending the atomic model to comprehend a third energy level. We introduce state  $|i\rangle_\beta$  whose parity is opposite to that of  $|e\rangle_\beta$ . For example, as we did above, a possible choice for the atomic levels can be  $|i\rangle \leftrightarrow \mu_i = 51$ ,  $|e\rangle \leftrightarrow \mu_e = 50$ ,  $|g\rangle \leftrightarrow \mu_g = 49$ .

If we set the cavity mode  $B$  resonant to  $|e\rangle \leftrightarrow |i\rangle$  the cavity field results out of resonance with  $|g\rangle \leftrightarrow |e\rangle$  and transitions at this frequency are strongly suppressed. Thus, setting resonance between atom  $\beta$  and cavity mode  $B$  for a time sufficient to realize a  $2\pi$ -Rabi pulse between  $|e1\rangle_{\beta B}$  and  $|i0\rangle_{\beta B}$ , state  $|e1\rangle_{\beta B}$  will acquire a  $-1$  phase factor [15, 43]. The phases of the other states that appear in (33) are not modified: the phases of  $|g0\rangle_{\beta B}$  and  $|g1\rangle_{\beta B}$  are unchanged because of the frequency mismatch while that of  $|e0\rangle$  does not change because it is an eigenstate of the Jaynes-Cummings Hamiltonian in the bidimensional Hilbert space spanned by  $\{|e\rangle, |i\rangle\}_\beta$ . We are, thus, able to perform transformations (34) and the state in Eq. (33) changes into:

$$ia|g\rangle_\beta \otimes (c|11\rangle + d|10\rangle)_{AB} + b|e\rangle_\beta \otimes (c|01\rangle - d|00\rangle)_{AB} \quad (35)$$

apart from a global phase factor.

Now, we need the set of transformations, on the system  $\beta + B$ , defined in Step 6 of the previous protocol. This make us obtain the final state:

$$\begin{aligned} i|g\rangle_\beta \otimes (ac|11\rangle + ad|10\rangle - bc|01\rangle + bd|00\rangle)_{AB} + \\ |e\rangle_\beta \otimes (ac|11\rangle + ad|10\rangle + bc|01\rangle - bd|00\rangle)_{AB}. \end{aligned} \quad (36)$$

If the measurement outcome of atom  $\beta$  is  $|e\rangle_\beta$ , the joint state of the two cavities is such that the action of the  $\pi$ -CQPG on qubits  $A$  and  $B$  is evident. If the outcome of the measurement is  $|g\rangle_\beta$ , we apply a  $2\pi$ -Rabi pulse for transition  $|g1\rangle_{\alpha A} \leftrightarrow |e0\rangle_{\alpha A}$  on system  $\alpha + A$ . It is relevant to notice that, in order to realize the local quantum phase gate of the protocol, just simple resonant Rabi oscillation in a atom-cavity system is required.

We have proposed a non-local  $\pi$ -CQPG between spatially separated cavities. Implementing a non-local CQPG is an important result, in quantum distributed computation, since it can help us in improving the efficiency of the non-local CNOT. The non ideality of Step 5 of the scheme for the CNOT $_{AB}$  strongly limits the efficiency of the gate. Since a CNOT operation can be simulated using a Hadamard transform on the target qubit followed by a  $\pi$ -CQPG, and the efficiency of implementation of a non-local  $\pi$ -CQPG is evidently better than that of the CNOT, the reliability of the non-local gate can be significantly improved.

In this case, however, the time needed to accomplish the entire non-local CNOT can represent a problem. The realization of a Hadamard transform of the cavity field requires a map of the quantum state of the field onto the relative ancillary (atomic) qubit. The performance of a Hadamard transform on the latter and, eventually, a map of the transformed state back onto the cavity qubit. This increases the time necessary to accomplish the non-local CNOT $_{AB}$  and the number of local transformations involved.

## VI. CONCLUSIONS

In this paper we have proposed a CQED set-up for the implementation of a non-local CNOT and of a non-local  $\pi$ -CQPG. According to the optimal theoretical protocols described in ref. [5], our experimental schemes use just two bits of classical communication and a single ebit, shared by the two parties.

The computational register, in the proposed set-up, is formed by two spatially separated microwave cavities while the required ebit is encoded in the entangled state of two Rydberg atoms.

For the case of the non-local CNOT, we have analyzed in full details the theoretical procedures and the experimental requirements needed to implement the gate in our CQED system. Our analysis has shown that some practical problems have to be taken in consideration in the proposed experimental scenario.

In particular, some difficulties arise connected with the low efficiency of the currently available sources of single-photon states operating in microwaves. On the other hand, while a local CNOT *cavity*  $\rightarrow$  *atom* can be efficiently realized via a controlled interaction of the atom with an external field, the practical implementation of a CNOT *atom*  $\rightarrow$  *cavity* is basically an inefficient operation. This low efficiency is due to the fact that the real-

ization of this local gate passes through an atomic transition that is forbidden by the electric-dipole-transitions selection rules. To circumvent this problem, we have proposed to set an externally driven two-photon transition between two suitably chosen states of the dressed-atom eigenspectrum. With this solution, we have found a significant improvement of the fidelity of the gate. We want to stress that the discussed difficulties are just related to the current *state of the art*: once these realizative problems will be solved, our experimental proposal will certainly acquire practical reliability.

The versatility of the proposed set-up has been shown describing how to modify the protocol for a non-local CNOT to get a non-local  $\pi - \text{CQPG}$ . The realization of this gate is based on atom-external field interactions of the kind used to implement a CNOT *cavity*  $\rightarrow$  *atom* and on resonant atom-cavity mode interactions. Because of the intrinsic high reliability of these operations, we have found that this non-local gate could be implemented in

an efficient way.

Despite the encountered difficulties to manage, the proposed set-up gives some insights in the fundamental research of possible architectures for a quantum computer able to manage large computational registers.

### Acknowledgments

We would like to thank T. Calarco, Byoung S. Ham, D. Vitali, A. Carollo and H. Jeong for helpful discussions. This work was supported by ESF under "Quantum Information Theory and Quantum Computing" program, by the EU under grants IST - EQUIP, "Entanglement in Quantum Information Processing and Communication" and by the UK Engineering and Physical Science Research Council through GR/R33304.

- 
- [1] G.M. Palma, K.-A. Suominen and A. K. Ekert *Proc. Roy. Soc. London A* **452**, 567 (1996).
- [2] D. P. DiVincenzo, D. Loss, *Superlattices and Microstructures* **23**, 419 (1998), LANL e-print: cond-mat/9710259.
- [3] D. P. DiVincenzo, *Phys. Rev. A* **50**, 1015 (1995),
- [4] J. I. Cirac, A. K. Ekert, S. F. Huelga, C. Macchiavello, *Phys. Rev. A* **59**, 4249 (1999).
- [5] J. Eisert, K. Jacobs, P. Papadopoulos, M. B. Plenio, *Phys. Rev. A* **62**, 52317 (2000), LANL e-print: quant-ph/0005101.
- [6] D. Collins, N. Linden, S. Popescu, *Phys. Rev. A* **64**, 32302 (2001), LANL e-print: quant-ph/0005102.
- [7] J. Preskill, *Lecture Notes for Physics 229: Quantum Information and Computation*, California Institute of Technology (1998), e-print: www.theory.caltech.edu/preskill/ph229.
- [8] M. A. Nielsen, I. L. Chuang *Quantum computation and quantum information* (Cambridge University Press, Cambridge, 2000).
- [9] C. Macchiavello, G. M. Palma and A. Zeilinger, *Quantum computation and quantum information theory*, (World Scientific, Singapore, 2001)
- [10] A. Ekert, P. Hayden, H. Inamori, LANL e-print: quant-ph/0011013.
- [11] V. Vedral, M. B. Plenio, LANL e-print: quant-ph/9802065.
- [12] J. Jang, J. Lee, M. S. Kim and Y. L. Park, LANL e-print: quant-ph/0101107.
- [13] S. Haroche and J. M. Raimond, in *Advanced in Atomic and Molecular Physics*, vol. **20**, D. R. Bates and B. Bederson eds., Academic Press, (1985); P. Domokos, J. M. Raimond, M. Brune, and S. Haroche, *Phys. Rev. A* **52**, 3554 (1995); A. Rauschenbeutel, G. Nogues, S. Osnaghi, P. Bertet, M. Brune, J. M. Raimond, S. Haroche, *Science* **288**, 2024 (2000).
- [14] M. Brune, J. M. Raimond, and S. Haroche, *Phys. Rev. A* **35**, 154 (1987)
- [15] V. Giovannetti, D. Vitali, P. Tombesi, A. Ekert, *Phys. Rev. A* **62**, 32306 (2000).
- [16] E. T. Jaynes, F. W. Cummings, *Proc. IEEE* **51**, 89 (1963).
- [17] H. J. Lee, C. S. Adams, M. Kasevich, S. Chu *Phys. Rev. Lett.* **76**, 2658 (1996).
- [18] W. D. Phillips, in *Les Houches Proceedings, Session LIII: Systems Fondamentaux en Optique Quantique*, J. Dalibard, J. M. Raymond and J. Zinn-Justin, eds. (1991).
- [19] S. Chu, J. E. Bjorkholm, A. Ashkin, A. Cable *Phys. Rev. Lett.* **57**, 314 (1986).
- [20] K. M. O'Hara, S. R. Granade, M. E. Gehm, T. A. Savard, S. Bali, C. Freed, J. E. Thomas, *Phys. Rev. Lett.* **82**, 4204 (1999).
- [21] J. Ye, W. Verwooy, H. J. Kimble, *Phys. Rev. Lett.* **83**, 4987 (1999).
- [22] R. J. C. Spreeuw, C. Gerz, L. S. Goldner, W. D. Phillips, S. L. Rolston, C. I. Westbrook, M. W. Reynolds, and I. F. Silvera, *Phys. Rev. Lett.* **72**, 3162 (1994);
- [23] C. C. Agosta, I. F. Silvera, H. T. C. Stoof, and B. J. Verhaar, *Phys. Rev. Lett.* **62**, 2361 (1989).
- [24] R. Dumke, M. Volk, T. Mütther, F. B. J. Buchkremer, G. Birkl, and W. Ertmer, *Phys. Rev. Lett.* **89**, 097903 (2002); F.B.J. Buchkremer, R. Dumke, M. Volk, T. Mütther, G. Birkl, W. Ertmer, *Laser Physics*, **12**, 736 (2002); G. Birkl, F.B.J. Buchkremer, R. Dumke, W. Ertmer, *Optics Comm.*, **191**, 67 (2001).
- [25] R. G. Brewer, in *Non Linear Optics*, P. G. Harper and B. S. Wherrett eds., Accademic Press, (1977).
- [26] M. Weissbluth *Atoms and Molecules* Academic Press (1994).
- [27] J. M. Raimond, M. Brune and S. Haroche *Rev. Mod. Phys.* **73**, 565 (2001).
- [28] A. Kühn, M. Hennrich and G. Rempe, *Phys. Rev. Lett.* **89**, 067901 (2002); R. Brouri, A. Beveratos, J.-P. Poizat, and P. Grangier *Opt. Lett.* **25**, 1294 (2000); M. Pelton, C. Santori, G.S. Solomon, O. Benson and Y. Yamamoto, *Eur. Phys. J. D* **18**, 179 (2002); A. Beveratos, S. Kühn, R. Brouri, T. Gacoin, J.-P. Poizat and P. Grangier, *Eur. Phys. J. D*, pg. 191; W.L. Barnes, G. Björk, J.M. Gerard, P. Jonsson, J.A.E. Wasey, P.T. Worthing and V. Zwiller,

- Eur. Phys. J. D*, pg. 197.
- [29] M. Bourennane, F. Gibson, A. Karlsson, A. Hening, P. Jonsson, T. Tsegaye, D. Ljunggen, E. Sundberg, *Opt. Expr.* **4**, 383 (1999).
- [30] S. M. Tan, D. F. Walls, M. J. Collett *Phys. Rev. Lett.* **66**, 252 (1991).
- [31] C. K. Hong and L. Mandel, *Phys. Rev. Lett.* **56**, 58 (1986).
- [32] D. N. Klyshko, *Sov. Phys. JETP* **28**, 522 (1969); D. C. Burnham and D. L. Weinberg, *Phys. Rev. Lett.* **25**, 84 (1970).
- [33] J. G. Rarity and P. R. Tapster, *Phys. Rev. Lett.* **64**, 2495 (1990).
- [34] J. I. Cirac, P. Zoller, H. J. Kimble, and H. Mabuchi, *Phys. Rev. Lett.* **78**, 3221 (1997).
- [35] S. Brattke, B. T. H. Varcoe, and H. Walther, *Phys. Rev. Lett.* **86**, 3534 (2001).
- [36] M. Fleischhauer and M. D. Lukin, *Phys. Rev. Lett.* **84**, 5094 (2000); S. E. Harris, *Phys. Today* **50**, 36 (1997).
- [37] This multichannel read-out has been very recently demonstrated in a neat experiment by A. S. Zibrov *et al.* *Phys. Rev. Lett.* **88**, 103601 (2002).
- [38] We acknowledge the contribution given by B. S. Ham about this point.
- [39] P. Goy, L. Moi, M. Gross, J. M. Raimond, C. Fabre,, and S. Haroche *Phys. Rev. A* **26**, 2065 (1982); J. R. Tucker and M. J. Feldman, *Rev. Mod. Phys.* **57**, 1055-1113 (1985).
- [40] S. Haroche, in *Les Houches Proceedings, Session LIII: Systems Fondamentaux en Optique Quantique*, J. Dalibard, J. M. Raymond and J. Zinn-Justin eds. (1991).
- [41] C. Cohen Tannoudji, B. Diu, F. Laloë, *Quantum Mechanics* (J. Wiley & sons, 1977).
- [42] C. Cohen-Tannoudji, J. Dupont-Roc, G. Grynberg *Atom-Photon Interactions* (John Wiley & Sons, 1992).
- [43] A. Rauschenbeutel, G. Nogues, S. Osnaghi, P. Bertet, M. Brune, J. M. Raimond, S. Haroche, *Phys. Rev. Lett.* **83**, 5166 (1999).
- [44] Circularity means that the angular quantum number of each considered level is maximum:  $l = \mu - 1$ .
- [45] This explains how to realize an efficient  $\pi$ -pulse that could exchange  $|0g\rangle_{B\beta}$  and  $|0e\rangle_{B\beta}$  as required, on the state of system  $A + B + \beta$ , after a measurement having  $|e\rangle_{\alpha}$  as output.